Trinity College Dublin
Coláiste na Tríonóide, Baile Átha Cliath
The University of Dublin

School of Engineering
Faculty of Engineering, Mathematics & Science
Trinity College Dublin

4B4 Heat Transfer

Heat Exchanger Lab Report

Group members	Finn O'Connor, Max Riome, Angus Seigne, Sophie Howard, Ulaş Ima
Laboratory group	Mech-14
Date of lab session	18/11/2025
Date of submission	02/12/2025

I have read and I understand the plagiarism provisions in the General Regulations of the University Calendar for the current year, found at http://www.tcd.ie/calendar.

FINN O'CONNOR Max Riome Angus seigne Ulaş Ima Sophie Howard

SIGNATURES

I have also completed the Online Tutorial on avoiding plagiarism 'Ready Steady Write', located at http://tcd-ie.libguides.com/plagiarism/ready-steady-write.

FINN O'CONNOR Max Riome Angus seigne Ulaş Ima Sophie Howard

SIGNATURES

1 Abstract

This experiment is conducted to investigate the thermal characteristics of a cross-flow water to air recuperative heat exchanger. The influence of fluid mass flow rates on heat transfer, heat loss and overall heat transfer coefficient is investigated. The experimental setup involves twelve test conditions, using three water mass flow rates $\dot{m}_{\text{w}}$ and four air mass flow rates $\dot{m}_{\text{a}}$. Average temperatures and flow rates were recorded two minutes after the thermal equilibrium was achieved for each iteration of the experiment. From the collected data, uncertainties, heat transfer rates on water and air sections (Q_w and Q_a), percentage heat loss, logarithmic mean temperature differences (LMTD) and overall heat transfer coefficients were calculated.

The results displayed a somewhat proportional relationship between air mass flow rate and heat transfer rates for most calculated quantities. Q_w tended to decrease with increased $\dot{m}_{\text{w}}$while increasing with higher $\dot{m}_{\text{a}}$, and the inverse was observed for Q_a. The heat transfer coefficient U increased gradually with both higher $\dot{m}_{\text{w}}$ and $\dot{m}_{\text{a}}$. The percentage heat losses were negative, measurement 9 even reaching -61.697% meaning the fluid gained heat energy during transfer rather than losing energy to the surrounding environment. It was concluded that this was a direct result of fluid frictional forces. To confirm measurement consistencies, a repeatability test was carried out based on measurement 7. The results of this test showed some correlation with the iteration on which it was based, the inaccuracies were attributed to drift in the Pt100 sensors and thermal fluctuations. The experiment was deemed repeatable.

2 Introduction and Objectives

Heat exchangers are devices used to transfer thermal energy between two or more fluids at different temperatures while in thermal contact. They are typically made up of heat exchanging elements, such as core/matrix, that provide the heat transfer surface, and fluid distribution elements such as headers, manifolds or inlet and outlet nozzles. These types of machinery serve a wide range of applications, from steam generation in petroleum industries, to condensers/oil coolers in power plants and moreover in refrigeration and air conditioning for space heating industries.

Although heat exchangers are found in multiple forms, they are fundamentally grouped into three basic types, recuperators, regenerators and direct contact heat exchangers. Recuperators are the most common type and are direct transfer heat exchangers, where fluids are separated by a heat-transfer surface. Ideally, said fluids do not mix or leak. In contrast, regenerators are indirect transfer heat exchangers, in which, an intermittent heat exchange takes place between the fluids via thermal energy storage and release through the exchanger surface/matrix. Due to varying pressure differences and matrix rotation/valve switching, regenerators exhibit the tendency of fluid leakage from one stream to another [1]. Lastly, the direct contact heat exchangers transfer heat via the contact between two process streams. While they are able to be used for the majority of systems and offer economic advantages over other types of exchangers, their practicality can be limited by their complexity [2].

Heat exchangers could also be classified according to their geometries into four categories: double pipe, cross flow, shell and tube and compact heat exchangers [3]. In this experimental analysis, a recuperative heat exchanger is used to achieve its objective of characterising the performance of a cross-flow water to heat exchanger.

3 Background and Theory

The basis of this experiment stems from the First Law of Thermodynamics for an ideal, adiabatic system, assuming no heat loss.

$$Q_w = Q_a \tag{1}$$

Where: $Q_w = \dot{M}_w \, c_{p,w} \, (T_{w,in} - T_{w,out}) \qquad and \qquad Q_a = \dot{M}_a \, c_{p,a} \, (T_{a,out} - T_{a,in})$

However, accounting for heat losses, $Q_w = Q_a + Q_{loss}$. The percentage heat losses can be calculated as:

$$Q_{loss} \, (\%) = \frac{(Q_w - Q_a}{Q_w} \times 100 \tag{2}$$

Fluid frictional losses should also be taken into account for the case of the experiment. They may cause an increase in the fluid temperature, proportional to the pressure drop encountered in the system.

Newton's Law of Cooling:

$$Q_{cnv} = \frac{\Delta T}{R_t} = UA\Delta T_{LM} \approx Q_a \tag{3}$$

For this particular setup $A = 0.0317$ m^2. The convective heat transfer can either be measured as the energy increase in the air stream (Q_a) or an energy decrease in the water stream.

For a cross-flow heat exchanger, the logarithmic mean temperature difference (T_{LM} can be modelled using the counter-flow heat exchanger approach for ΔT_1 ($T_{w,in} - T_{a,out}$) and ΔT_2 ($\Delta T_{T_w,out} - T_{a,in}$) and applying a correction factor, F.

$$\Delta T_{LM} = F \cdot \frac{\Delta T_1 - \Delta T_2}{\ln\left(\frac{\Delta T_1}{\Delta T_2}\right)} \tag{4}$$

Where F depends on the four temperatures $T_{w,in}, T_{w,out}, T_{a,in}$, and $T_{a,out}$. To accurately attain F values, exact values of P and accurate values of Z were plotted using a web plot digitiser, where:

$$P = \frac{t_o - t_i}{T_i - T_o}, \qquad Z = \frac{T_i - T_o}{t_i - t_o} \tag{5}$$

4 Experimental Setup, Data Processing, and Uncertainty Analysis

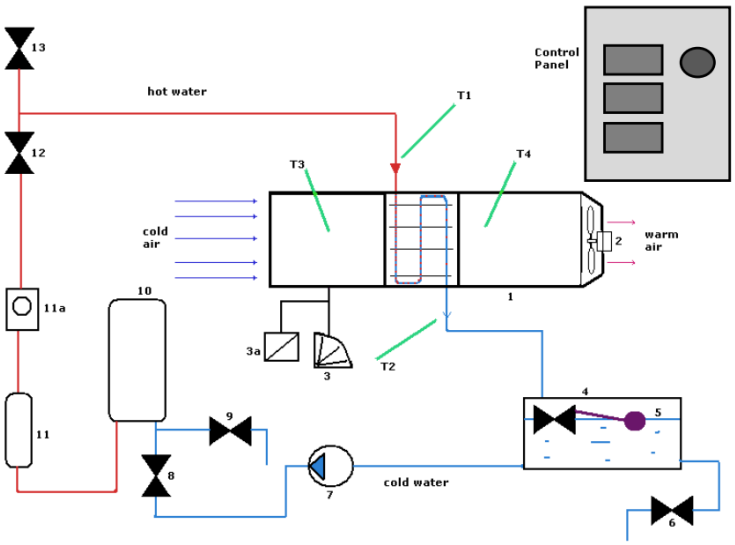

ID	Component
1	Testing tunnel
2	Variable speed fan
3, 3a	Differential micro manometers
4	Water reservoir
5	Float valve
6	Reservoir discharge valve
7	Three-speed water circulation pump
8	Boiler safety valve
9	Boiler discharge valve
10	Electric boiler/heater, set to approximately 60 °C
11	Rotameter flow meter (0-300 L/h)
11a	Turbine type digital flow meter
12	Flow control valve
13	Air bleed valve
14	Control Panel

Figure 1: Schematic of the cross-flow heat exchanger apparatus.

4.1 Experimental Setup

The experimental setup consisted of a crossflow water to air heat exchanger and a computer for the data acquisition. The heat exchanger had two inlets and two outlets each for water and air, where temperatures were taken by Pt100 temperature probes at each inlet/outlet, connected to the digital instruments.

The water and air flows were adjusted respectively via a valve and the control panel, where flow rates were displayed for both fluids. A rotometer is also present in the system, however the water flow rate was tracked from the control panel for better accuracy. It was decided to have 12 measurements taken down, with 3 different water flowrates and 3 different air flowrates. Firstly a null measurement was run to determine the offset of differential pressure to obtain corrected pressures to calculate the air flow rates. After setting the variables to the desired values from the control panel, the data acquisition process was initiated from the computer.

The data was then downloaded to an excel file. The data after the convergence was assumed to be in thermal equilibrium and data before convergence were discarded. Two minutes of data was later analysed, starting after convergence to ensure accuracy. This experimental process was repeated with different flow rate values for 12 measurements. After the experiment, an uncertainty analysis was carried out, moreover a heat loss and overall heat transfer coefficient (U) was calculated and plotted. Lastly, the effect of different flow rates on heat transfer performance were analysed.

Table 1: Recorded air and water flow rate combinations.

Air flow rate (kg/h)	Water flow rate (L/h)
50	100
100	100
150	100
200	100
50	150
100	150
150	150
200	150
50	200
100	200
150	200
200	200

For repeatability measurement 7, where the flow rates are 150 kg/h and 150 L/h respectively for air and water, was re-run and results were compared with the previous run. Only slight offsets were displayed that would not drastically affect the results, ensuring repeatability. An uncertainty analysis was then conducted, where for the primary measured quantities, averages and standard deviations were calculated with the respective equations given below; where μ_i is the average, and σ_i is the standard deviation of N measurements of a X, which is a quantity such as temperature or flow rate.

Average:

$$\mu_X = \frac{1}{N}\sum_{i=1}^{N} X_i \tag{6}$$

Standard deviation:

$$\sigma_X = \left(\frac{1}{N-1}\sum_{i=1}^{N}(X_i - \mu_X)^2\right)^{1/2} \tag{7}$$

The absolute uncertainty, U_X , was then calculated, taking into account that the data acquisition system is updated every 5 seconds. Furthermore it is assumed that the data acquisition measurements are normally distributed with a confidence level of 95%, the equation for the absolute certainty is given below.

$$U_X = t_{95\%,N-1}\frac{\sigma_X}{\sqrt{N}} \tag{8}$$

Where N in this case is the number of statistically independent samples, and $t_{95\%,N-1}$ is the inverse of the cumulative t-distribution for a confidence level of 95%. After calculating these uncertainties and assuming all variables are statistically independent, the following uncertainty propagation rules are applied.

Addition and subtraction of X_1 and X_2:

$$U_{(x_1 \pm x_2)} = \left(U_{x_1}^2 + U_{x_2}^2\right)^{1/2} \tag{9}$$

Multiplication or division of X_1 and X_2:

$$u_{(x_1 \cdot x_2)} = u_{(x_1 \cdot x_2)} = \left(u_{x_1}^2 + u_{x_2}^2\right)^{1/2} \tag{10}$$

Scalar multiplication or division of X_1:

$$u_{(aX_1+b)} = aU_{(X_1)} \tag{11}$$

Scalar power of X_1:

$$u_{(aX_1^m)} = m \cdot u_{(x_1)} \tag{12}$$

Absolute uncertainty of a function:

$$U_{f(x_1 \cdot x_2)} = u_{(x_1 \cdot x_2)} = \left[(\frac{\delta f}{\delta X_1})^2 U_{X_1}^2 + (\frac{\delta f}{\delta X_2})^2 U_{X_2}^2 + \cdots\right]^{1/2} \tag{13}$$

Absolute uncertainty of logarithm of X_1:

$$U_{(ln_{X1})} = \frac{1}{X_1} U_{X_1)} \leftrightarrow u_{(ln_{X1})} = \frac{1}{X_1} \frac{U_{X_1}}{lnX_1} = \frac{u_{X_1}}{lnX_1} \tag{14}$$

To conclude the setup, the resulting values are quoted and the relative uncertainties are given in percentages. Also because 0 degrees Celsius is an arbitrary zero value in the temperature scale, the relative uncertainties for temperatures given in celsius were not quoted, aside from cases that involve temperature differences.

5 Uncertainty Analysis (Worked Example for Test 1)

In this section, the full uncertainty calculation is shown for a single operating point (Test 1). Each .T57 was first processed using MATLAB to give all temperature mean values and corresponding uncertainties. The results were plotted in an excel sheet which was set up to automatically compute all subsequent calculations and uncertainties. All of the following numerical values are taken directly from the processed Excel sheet. The following constants were used in the calculation processes:

Table 2: Thermophysical Properties Used in Calculations

Property	**Value**
Water Density (ρ_w)	999 kg/m^3
Water Specific Heat Capacity ($c_{p,w}$)	4184 J/(kg·K)
Air Specific Heat Capacity ($c_{p,a}$)	1004 J/(kg·K)
Heat Exchanger Surface Area (A)	0.317 m^2

5.1 Input Quantities

Steady–state temperatures:

$$T_1 = 57.848 \text{ K},$$
$$T_2 = 53.968 \text{ K},$$
$$T_3 = 19.384 \text{ K},$$
$$T_4 = 49.676 \text{ K}.$$

Absolute uncertainties (95% confidence, obtained from the data acquisition statistics):

$$U_{T_1} = 0.0414 \text{ K},$$
$$U_{T_2} = 0.0389 \text{ K},$$
$$U_{T_3} = 0.0307 \text{ K},$$
$$U_{T_4} = 0.0362 \text{ K}.$$

Relative temperature uncertainties:

$$u_{T_1} = \frac{U_{T_1}}{T_1} = \frac{0.0414}{57.848} = 7.15 \times 10^{-4} \approx 0.072\%,$$
$$u_{T_2} = \frac{0.0389}{53.968} = 7.21 \times 10^{-4} \approx 0.072\%,$$
$$u_{T_3} = \frac{0.0307}{19.384} = 1.58 \times 10^{-3} \approx 0.158\%,$$
$$u_{T_4} = \frac{0.0362}{49.676} = 7.29 \times 10^{-4} \approx 0.073\%.$$

Mass flow rates:

$$\dot{m}_w = 0.027778 \text{ kg/s},$$
$$U_{\dot{m}_w} = 0.000278 \text{ kg/s},$$
$$\dot{m}_a = 0.013889 \text{ kg/s},$$
$$U_{\dot{m}_a} = 0.000139 \text{ kg/s}.$$

Constants:

$$c_{p,w} = 4184 \text{ J/kgK}, \qquad c_{p,a} = 1004 \text{ J/kgK},$$

$$A = 0.0317 \text{ m}^2, \qquad F = 0.965.$$

5.2 Temperature Differences

The hot– and cold–side temperature differences used for the LMTD are

$$\Delta T_1 = T_1 - T_4 = 57.848 - 49.676 = 8.172 \text{ K},$$
$$\Delta T_2 = T_2 - T_3 = 53.968 - 19.384 = 34.584 \text{ K}.$$

Uncertainties are obtained using

$$U_{\Delta T} = \sqrt{U_{T_i}^2 + U_{T_j}^2}.$$

For ΔT_1:

$$U_{\Delta T_1} = \sqrt{U_{T_1}^2 + U_{T_4}^2} = \sqrt{(0.0414)^2 + (0.0362)^2} = 0.054995 \text{ K}.$$

Relative:

$$u_{\Delta T_1} = \frac{U_{\Delta T_1}}{\Delta T_1} = \frac{0.054995}{8.172} = 6.73 \times 10^{-3} = 0.673\%.$$

For ΔT_2:

$$U_{\Delta T_2} = \sqrt{U_{T_2}^2 + U_{T_3}^2} = \sqrt{(0.0389)^2 + (0.0307)^2} = 0.04955 \text{ K}.$$

$$u_{\Delta T_2} = \frac{0.04955}{34.584} = 1.433 \times 10^{-3} = 0.143\%.$$

5.3 Heat Transfer Rates

5.3.1 Water Side

$$Q_w = \dot{m}_w c_{p,w}(T_1 - T_2).$$

$$T_1 - T_2 = 57.848 - 53.968 = 3.880 \text{ K}.$$

$$Q_w = 0.027778 \times 4184 \times 3.880 = 450.9422 \text{ W}.$$

Uncertainty in Q_w:

$$u_{Q_w} = \sqrt{\left(\frac{U_{\dot{m}_w}}{\dot{m}_w}\right)^2 + \left(\frac{U_{T_1-T_2}}{T_1 - T_2}\right)^2}$$

$$U_{Q_w} = u_{Q_w}\, Q_w$$

$$u_{Q_w} = \sqrt{\left(\frac{0.000278}{0.027778}\right)^2 + \left(\frac{0.054995}{3.880}\right)^2} = 0.01746$$

$$U_{Q_w} = 0.01746 \times 450.9422 = 6.602 \text{ W}$$

5.3.2 Air Side

$$Q_a = \dot{m}_a c_{p,a}(T_4 - T_3).$$

$$T_4 - T_3 = 49.676 - 19.384 = 30.292 \text{ K}$$

$$Q_a = 0.013889 \times 1004 \times 30.292 = 422.4051 \text{ W}$$

Uncertainty:

$$u_{Q_a} = \sqrt{\left(\frac{U_{\dot{m}_a}}{\dot{m}_a}\right)^2 + \left(\frac{U_{T_4-T_3}}{T_4 - T_3}\right)^2}$$

$$U_{Q_a} = u_{Q_a}\, Q_a$$

$$u_{Q_a} = \sqrt{\left(\frac{0.000139}{0.013889}\right)^2 + \left(\frac{0.04955}{30.292}\right)^2} = 0.01013$$

$$U_{Q_a} = 0.01013 \times 422.4051 = 0.6619 \text{ W}$$

5.4 Percentage Heat Loss

$$\%\text{loss} = \frac{Q_w - Q_a}{Q_w} \times 100.$$

$$Q_w - Q_a = 450.9422 - 422.4051 = 28.5371 \text{ W}$$

$$\%\text{loss} = \frac{28.5371}{450.9422} \times 100 = 6.32833\%.$$

5.5 Logarithmic Mean Temperature Difference

For a cross–flow exchanger, the LMTD with correction factor F is

$$\Delta T_{\text{LM}} = F\left(\frac{\Delta T_1 - \Delta T_2}{\ln(\Delta T_1/\Delta T_2)}\right).$$

$$\Delta T_1 - \Delta T_2 = 8.172 - 34.584 = -26.412 \text{ K},$$

$$\frac{\Delta T_1}{\Delta T_2} = \frac{8.172}{34.584} = 0.2364,$$

$$\ln\left(\frac{\Delta T_1}{\Delta T_2}\right) = \ln(0.2364) = -1.443.$$

Hence

$$\Delta T_{\text{LM}} = 0.965\frac{-26.412}{-1.443} = 0.965 \times 18.310 = 17.66686 \text{ K}.$$

Uncertainty in ΔT_{LM}

$$U_{\Delta T_{\text{LM}}} = \sqrt{\left(\frac{\partial \Delta T_{\text{LM}}}{\partial \Delta T_1} U_{\Delta T_1}\right)^2 + \left(\frac{\partial \Delta T_{\text{LM}}}{\partial \Delta T_2} U_{\Delta T_2}\right)^2}$$

$$U_{\Delta T_{\text{LM}}} = \sqrt{(0.45413 \cdot 0.054995)^2 + (-0.17733 \cdot 0.04955)^2}$$

$$= 0.04997 \text{ K}$$

$$u_{\Delta T_{\text{LM}}} = \frac{0.04997}{17.66686} = 2.83 \times 10^{-3} = 0.283\%$$

5.6 Overall Heat Transfer Coefficient

$$U = \frac{Q_a}{A\,\Delta T_{\text{LM}}}.$$

$$A\Delta T_{\text{LM}} = 0.0317 \times 17.66686 = 0.5604 \text{ W/K}.$$

$$U = \frac{422.4051}{0.5604} = 754.2417 \text{ W/m}^2\text{K}.$$

and ΔT_{LM}:

$$u_U = \sqrt{\left(\frac{U_{Q_a}}{Q_a}\right)^2 + \left(\frac{U_{\Delta T_{\text{LM}}}}{\Delta T_{\text{LM}}}\right)^2}.$$

$$\frac{U_{Q_a}}{Q_a} = \frac{0.661874}{422.4051} = 1.567 \times 10^{-3},$$

$$\frac{U_{\Delta T_{\text{LM}}}}{\Delta T_{\text{LM}}} = \frac{0.049967}{17.66686} = 2.83 \times 10^{-3}.$$

$$u_U = \sqrt{(1.567 \times 10^{-3})^2 + (2.83 \times 10^{-3})^2} = 0.324\%.$$

$$U_U = u_U\, U = 0.00324 \times 754.2417 = 2.44 \text{ W/m}^2\text{K}$$

6 Results and Discussion

The performance of the cross-flow heat exchanger was assessed through four main quantities: percentage heat loss, overall heat transfer coefficient U, airstream heat transfer Q_a, and water-side heat transfer Q_w. These were evaluated over a range of air and water mass flow rates to identify the dominant factors governing thermal performance.

6.1 Graphed Measurement Results

Eight plots were generated to illustrate how the key parameters change with $\dot{m}_a$ and $\dot{m}_w$. Across all measurements, air mass flow rate had the strongest influence on heat transfer behaviour, while changes in water flow primarily affected the measured temperature differences and uncertainty.

6.1.1 Percentage Heat Loss vs Mass Flow Rate ($\dot{m}$)

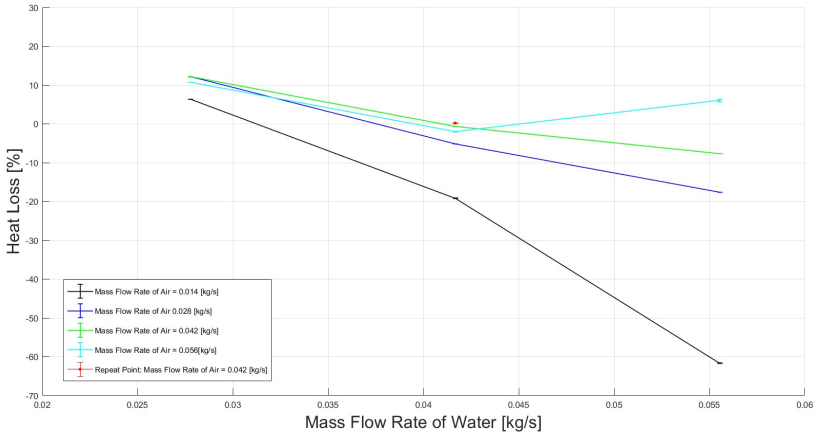

Figure 2: Percentage Heat Loss vs $\dot{m}_{\text{w}}$ with varied $\dot{m}_{\text{a}}$.

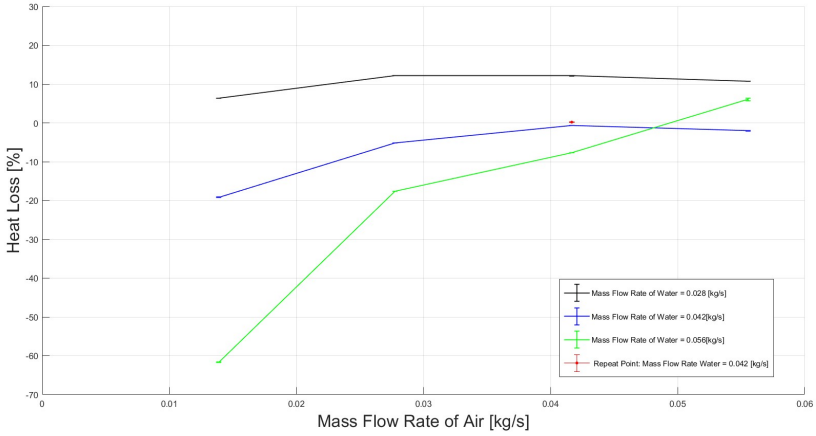

Figure 3: Percentage Heat Loss vs $\dot{m}_{\text{a}}$ with varied $\dot{m}_{\text{w}}$.

Percentage heat loss decreased with increasing water mass flow rate for all air-flow conditions. Higher $\dot{m}_w$ reduces the water temperature drop, causing Q_w to fall and in some cases become smaller than Q_a, producing negative apparent losses due to the high sensitivity of Q_w to small ΔT_w values.

Increasing air mass flow rate produced the opposite trend: heat loss increased because Q_a rose more rapidly than Q_w. This reflects the dominant role of air-side convection, as air velocity (and thus Reynolds number) increases significantly even for small changes in $\dot{m}_a$.

6.1.2 Heat Transfer Coefficient (U) vs Mass Flow Rate ($\dot{m}$)

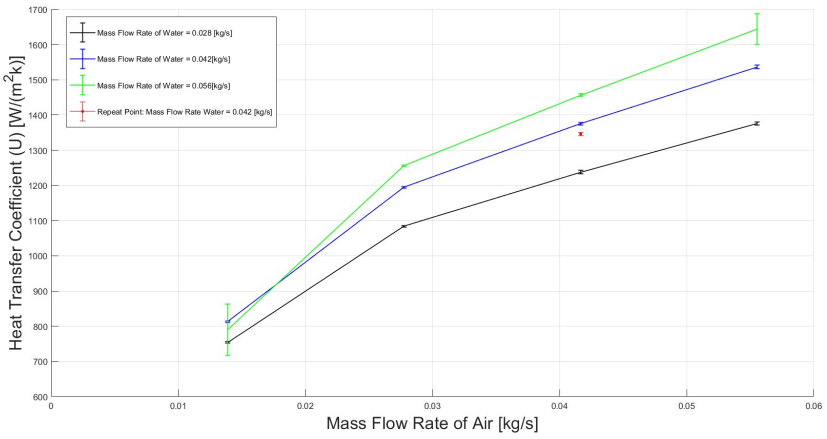

Figure 4: U vs $\dot{m}_{\text{a}}$ with varied $\dot{m}_{\text{w}}$.

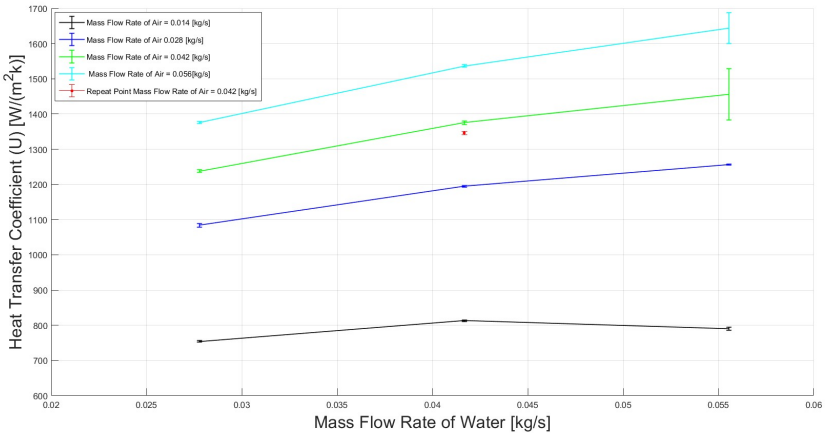

Figure 5: U vs $\dot{m}_{\text{w}}$ with varied $\dot{m}_{\text{a}}$.

The heat transfer coefficient increased strongly with air mass flow rate and only weakly with water mass flow rate. This is consistent with the thermal resistance network:

$$U^{-1} = h_w^{-1} + R_{\text{wall}} + h_a^{-1}, \tag{15}$$

where the air-side convection coefficient h_a provides the dominant resistance. Since $h_a \propto Re^{0.8} \propto \dot{m}_a^{0.8}$ (Dittus–Boelter correlation), increasing $\dot{m}_a$ sharply increases U. In contrast, increasing $\dot{m}_w$ reduces water-side resistance only slightly, resulting in relatively flat curves. Minor scatter appears at high $\dot{m}_w$ where ΔT_w is small and uncertainty increases.

6.1.3 Airstream Heat (Q_a) vs Mass Flow Rate ($\dot{m}$)

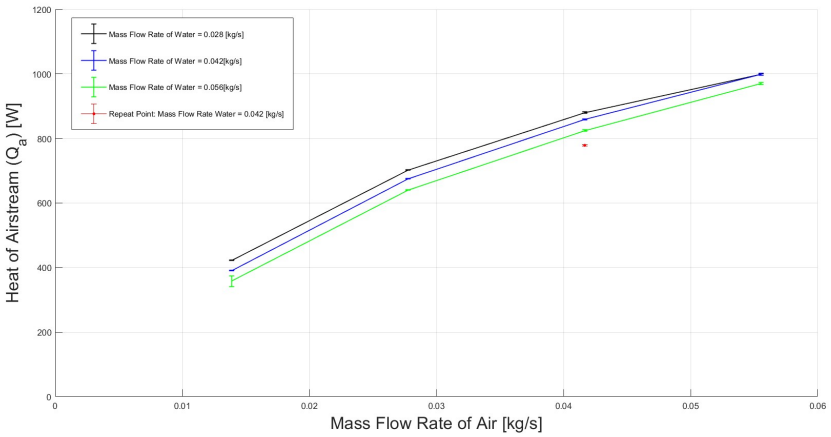

Figure 6: Q_a vs $\dot{m}_{\text{a}}$ with varied $\dot{m}_{\text{w}}$.

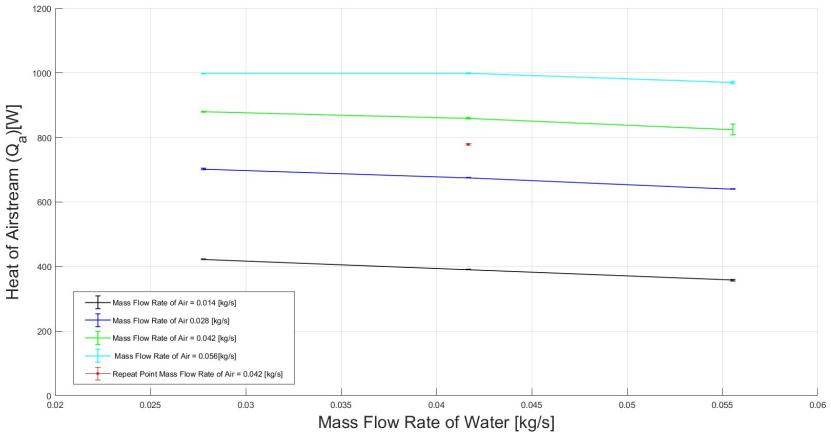

Figure 7: Q_a vs $\dot{m}_{\text{w}}$ with varied $\dot{m}_{\text{a}}$.

Q_a increased nearly linearly with air mass flow rate, reflecting the corresponding increase in air-side convection. For all water-flow conditions, Q_a rose from approximately 350–400 W at $\dot{m}_a = 0.014$ kg/s to around 900–1000 W at $\dot{m}_a = 0.056$ kg/s. Varying water flow had little effect on Q_a, again highlighting the dominant influence of the air side.

6.1.4 Water-Side Heat (Q_w) vs Mass Flow Rate ($\dot{m}$)

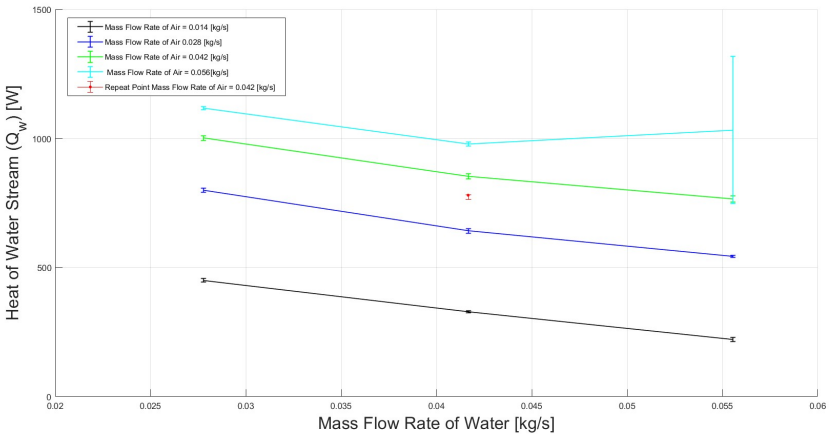

Figure 8: Q_w vs $\dot{m}_{\text{a}}$ with varied $\dot{m}_{\text{w}}$.

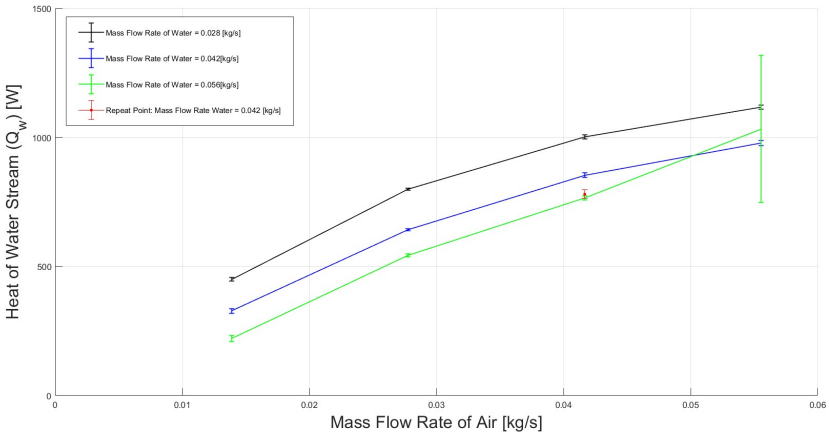

Figure 9: Q_w vs $\dot{m}_{\text{w}}$ with varied $\dot{m}_{\text{a}}$.

Q_w increased with air mass flow rate because stronger air-side convection increases heat extraction from the water. When water mass flow rate increased at fixed air flow, Q_w decreased due to the strong reduction in ΔT_w. At the highest water flows, scatter was observed due to the very small ΔT_w values amplifying uncertainty.

6.2 Repeatability Analysis

A repeat measurement of Test 7 ($\dot{m}_w = \dot{m}_a = 0.042$ kg/s) was performed and is shown as the red point in all plots. The original test produced:

$$Q_w = 853.6 \text{ W}, \qquad Q_a = 859.4 \text{ W},$$

while the repeat produced:

$$Q_w = 780.3 \text{ W}, \qquad Q_a = 778.8 \text{ W}.$$

Air-side values agreed within 10%, while water-side variation was moderately larger due to sensitivity to ΔT_w. Percentage heat loss differed only slightly (-0.686% vs 0.198%), showing that heat balance remains consistent. Overall, the repeatability was acceptable, and deviations can be attributed to:

- Thermal fluctuations in the heater.
- Drift in the Pt100 sensors.
- Increased sensitivity when ΔT_w is small.

6.3 Results Tables

Table 3: Summary of Results

Test	$\dot{m}_w$ [kg/s]	$\dot{m}_a$ [kg/s]	Q_w [W]	Q_a [W]	$Q_{loss}[\%]$
1	0.028	0.014	450.942 $\pm$ 6.602	422.405 $\pm$ 0.662	6.328 $\pm$ 0.0165
2	0.028	0.028	799.446 $\pm$ 3.994	702.502 $\pm$ 0.732	12.126 $\pm$ 0.0057
3	0.028	0.042	1001.743 $\pm$ 8.027	880.270 $\pm$ 2.692	12.126 $\pm$ 0.0092
4	0.028	0.056	1117.965 $\pm$ 7.399	998.422 $\pm$ 2.797	10.693 $\pm$ 0.0076
5	0.042	0.014	328.113 $\pm$ 9.006	390.992 $\pm$ 0.357	-19.164 $\pm$ 0.0302
6	0.042	0.028	642.244 $\pm$ 4.043	675.469 $\pm$ 0.597	-5.173 $\pm$ 0.0070
7	0.042	0.042	853.588 $\pm$ 8.689	859.445 $\pm$ 1.726	-0.686 $\pm$ 0.0114
8	0.042	0.056	978.847 $\pm$ 10.515	998.835 $\pm$ 2.629	-2.042 $\pm$ 0.0121
9	0.056	0.014	221.287 $\pm$ 12.146	357.814 $\pm$ 16.734	-61.697 $\pm$ 0.0655
10	0.056	0.028	543.920 $\pm$ 6.044	639.994 $\pm$ 0.846	-17.663 $\pm$ 0.0122
11	0.056	0.042	766.137 $\pm$ 8.408	824.786 $\pm$ 1.783	-7.655 $\pm$ 0.0122
12	0.056	0.056	1032.983 $\pm$ 284.379	970.310 $\pm$ 3.130	6.067 $\pm$ 0.3097
Repeat 7	0.042	0.042	780.316 $\pm$ 16.657	778.769 $\pm$ 1.636	0.198 $\pm$ 0.0239

Table 4: Summary of Outputs from Testing

Test	$\dot{m}_w$ [kg/s]	$\dot{m}_a$ [kg/s]	F	ΔT1 [k]	Error $\pm$ [k]	Δ T2 [k]	Error $\pm$ [k]
1	0.027778	0.013889	0.965	8.172	0.054995	34.584	0.049555
2	0.027778	0.027778	0.958	13.4822	0.027436	31.7929	0.033432
3	0.027778	0.041667	0.963	17.6308	0.070391	30.0539	0.062901
4	0.027778	0.055556	0.959	19.9731	0.062298	28.2539	0.051832
5	0.041667	0.013889	0.965	6.1142	0.045763	32.2714	0.035077
6	0.041667	0.027778	0.965	10.08	0.021391	30.616	0.023192
7	0.041667	0.041667	0.968	13.5333	0.047425	29.1815	0.044007
8	0.041667	0.055556	0.97	15.5851	0.057443	27.8777	0.050592
9	0.055556	0.013889	0.965	5.732	1.200685	30.44	0.033601
10	0.055556	0.027778	0.965	8.428	0.0247	29.036	0.031397
11	0.055556	0.041667	0.965	11.5	0.041959	27.92	0.036948
12	0.055556	0.055556	0.972	13.404	0.070644	26.356	1.222674
Repeat 7	0.041667	0.041667	0.972	12.584	0.095462	26.724	0.039327

7 Conclusions

This study investigated the thermal characteristics of a cross flow water to air recuperator. To understand how air and water flow rates affect thermal characteristics such as heat transfer, heat loss and overall heat transfer, twelve operating conditions were experimented with. It was shown from the results consistently that air mass flow rate, $\dot{m}_a$, played a dominant role regarding the exchanger's performance. It was observed that increasing Q_a led to higher airstream heat transfer rates and overall heat transfer coefficients, which shows that the air convection is strongly dependent on flow velocity. In contrast, increases in water mass flow rate, $\dot{m}_w$, have been seen to decrease the temperature drop across the water side, resulting in a decrease in Q_w, increasing uncertainties for smaller values of ΔT_w.

The results displayed negative heat losses of up to -61.697%, indicating heat energy was gained rather than dissipated to surroundings. This was possibly caused by smaller temperature differences on the water side, or frictional heating within the system.

The repeatability test that was performed on the seventh measurement provided inconsistencies with the data gathered from the earlier run, particularly on the water side, where small temperature differences led to higher variations. These inconsistencies were attributed to the errors induced by frictional forces, and thus the experiment was deemed repeatable.

Overall this experiment shows that air flow rate is a dominant factor relating to the performance of recuperative heat exchangers, and high water flow rates can reduce ΔT causing uncertainties to increase. These findings highlight the importance of accurate analysis of uncertainties when examining the behaviour of an exchanger.

References

[1] Dusan P. Sekulic and Ramesh K. Shah. *Fundamentals of Heat Exchanger Design*. John Wiley & Sons, November 2023. Google-Books-ID: YMjcEAAAQBAJ.

[2] Harold R. Jacobs. DIRECT CONTACT HEAT EXCHANGERS. In *Thermopedia*. Begel House Inc., February 2011.

[3] William S. Janna. *Engineering Heat Transfer, Second Edition*. CRC Press, December 1999. Google-Books-ID: g9u9pU8TDuAC.